Magnetic properties of cobalt-ferrite nanoparticles embedded in polystyrene resin

P. P. Vaishnava
Kettering University, Flint, Michigan 48504

U. Senaratne, E. Buc, and R. Naik
Department of Physics and Astronomy, Wayne State University, Detroit, Michigan 48201

V. M. Naik[a)]
University of Michigan-Dearborn, Dearborn, Michigan 48128

G. Tsoi and L. E. Wenger
University of Alabama, Birmingham, Alabama 35294

P. Boolchand
Department of ECECS, University of Cincinnati, Ohio 45221

(Presented on 1 November 2005; published online 20 April 2006)

Samples of maghemite and cobalt-ferrite nanoparticles (sizes, 3–10 nm) were prepared by cross-linking sulfonated polystyrene resin with aqueous solutions of (1) $FeCl_2$, (2) 80% $FeCl_2$ +20% $CoCl_2$, (3) $FeCl_3$, and (4) 80% $FeCl_3$+20% $CoCl_2$ by volume. Chemical analysis, x-ray powder-diffraction, and ^{57}Fe Mössbauer spectroscopic measurements show that samples 1 and 3 consist of γ-Fe_2O_3 nanoparticles (sizes, ~10 and 3 nm) and sample 2 and 4 consist of $Co_xFe_{3-x}O_4$ nanoparticles (sizes, ~10 and 4 nm). The temperature dependence of the zero-field-cooled and field-cooled magnetizations at low temperatures, together with a magnetic hysteresis in the M versus H data below blocking temperatures, demonstrate superparamagnetic behavior. The introduction of Co in the iron oxide-resin matrix results in an increase in the blocking temperature of nanoparticles.
 [DOI: 10.1063/1.2165922]

I. INTRODUCTION

Magnetic nanoparticles have attracted considerable attention in recent years due to their unique physical properties and potential industrial and biomedical applications.[1–3] Several methods have been reported in the literature to synthesize magnetic nanoparticles.[4] However, the ion-exchange method developed by Ziolo *et al.*[5] offers the distinct advantage of tolerating relatively lower temperatures (60–70 °C) and not producing particle aggregation. The memory effect and particle-size-dependent magnetic properties of γ-Fe_2O_3 precipitated in polystyrene and alginate hydrogel matrices prepared by this method have been studied in detail.[6–8] However, the ion-exchange method can also produce nanoparticles of ferrites and other structures. Progress has been made recently in spinel ferrite-based nanoparticles in the synthesis of specific magnetic carriers. In particular, size-controlled and antibody-coated ^{60}Co ferrite-based nanoparticles offer exciting possibilities for targeting neoplastic cells.[9,10]

In this paper we report synthesis of cobalt-ferrite nanoparticles by ion exchanging sulfonated polystyrene resin with iron and cobalt chlorides. The samples have been characterized by x-ray diffraction, ^{57}Fe Mössbauer spectroscopy, and superconducting quantum interference device (SQUID) magnetometry. The results clearly indicate dependence of the valence state of iron in the salt solutions and the amount of Co on the size and magnetic properties of the nanoparticles.

II. EXPERIMENT

Maghemite and cobalt-ferrite nanoparticles were prepared[5] by mixing 20 g of cross-linked sulfonated polystyrene resin with aqueous solutions of (1) $FeCl_2$, (2) 80% $FeCl_2$+20% $CoCl_2$, (3) $FeCl_3$, and (4) 80% $FeCl_3$ +20% $CoCl_2$. The solutions were then exposed to 1M solution of NaOH followed by dropwise addition of H_2O_2 (18% solution) at 65–70 °C. This process produced nanoparticles of iron oxide/ferrites of the first loading. The process was repeated several times to increase the amount of iron oxide/ferrite and the particle size. The sixth-loaded samples were characterized by chemical analysis, x-ray diffraction, ^{57}Fe Mössbauer spectroscopy, and SQUID magnetometry measurements. The atomic fractions of Fe and Co in samples

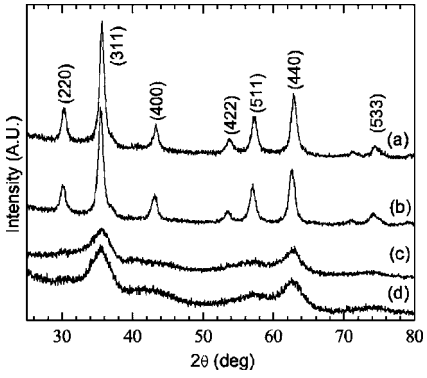

FIG. 1. X-ray-diffraction spectra for samples: (a) 1, (b) 2, (c) 3, and (d) 4. Samples 1 and 3 are without any Co. See text for sample description.

[a)]Electronic mail: vmnaik@umich.edu

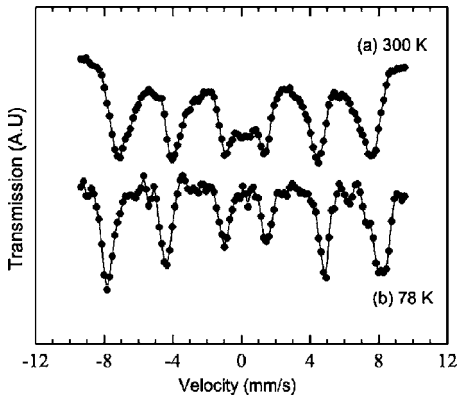

FIG. 2. ^{57}Fe Mössbauer spectra for sample 1: (a) at 300 K and (b) at 78 K.

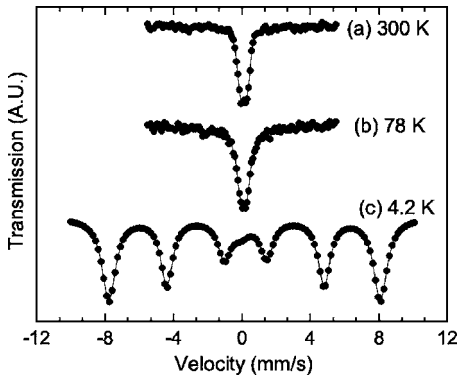

FIG. 3. ^{57}Fe Mössbauer spectra for sample 3 at (a) 300 K, (b) 78 K, and (c) 4.2 K.

were determined by chemical analysis using inductively coupled plasma atomic absorption spectroscopy.

III. RESULTS AND DISCUSSIONS

The x-ray powder-diffraction (XRD) patterns of samples 1–4 (see Fig. 1) show very similar peaks between 25° and 65°. However, the peaks for samples 3 and 4 were much broader than those for samples 1 and 2. The average particle size was calculated by using Scherer's equation. Based on the analysis, which included the peak positions and the peak intensities, the spectra were assigned as follows: sample 1, a single phase of γ-Fe_2O_3 (10 nm size), sample 2, a single phase of $Co_xFe_{3-x}O_4$ (x=0.6 and size of 10 nm), sample 3, a single phase of γ-Fe_2O_3 (3 nm), and sample 4, a single phase of $Co_xFe_{3-x}O_4$ (x=0.3 with particle size of 4 nm). The identification of the phases, especially for the samples 2 and 4, were difficult as the XRD patterns for γ-Fe_2O_3 and that for the $Co_{0.3}Fe_{2.7}O_4$ are very similar. However, as discussed in the following sections, the phases were identified tentatively through Mössbauer effect measurements.

The ^{57}Fe Mössbauer spectrum for sample 1 at room temperature shows [Fig. 2(a)] a doublet (quadrupole splitting 0.35 mm/s) superimposed on a broad six-line pattern (H_1 =482 kOe and H_2=443 kOe). The doublet corresponds to the superparamagnetic particles of γ-Fe_2O_3 and the six-line pattern due to the blocked or frozen moments of γ-Fe_2O_3 nanoparticles. When the sample is cooled to 78 K the doublet disappears and a magnetically split pattern with hyperfine fields of 517 and 488 kOe appears [Fig. 2(b)]. The values of the two fields correspond to the Fe^{3+} ions from the two sites of the γ-Fe_2O_3 structure. The Mössbauer spectrum of sample 2, containing Fe(II) and Co(II) ions, shows features resembling those of sample 1, except that the hyperfine fields at room temperature (492 and 453 kOe) and at liquid-nitrogen temperature (528 kOe) are larger than those in sample 1. The values of the hyperfine fields for sample 2 are indicative of a $Co_xFe_{3-x}O_4$ spinel phase[11] in the sample.

The Mössbauer spectra for sample 3 are shown in Fig. 3. At 300 K the spectrum [Fig. 3(a)] consists of a quadrupole doublet with splitting value of 0.35 mm/s corresponding to the superparamagnetic particles of γ-Fe_2O_3. Such a spectrum is characteristic of a high relaxation rate of the magnetic moment of the nanoparticles as compared to the Larmor precession of the iron nucleus. Upon cooling the sample to 78 K [Fig. 3(b)] some particles slow down (frozen moment) but not sufficient enough to exhibit a characteristic six-line Mössbauer pattern. At 4.2 K, however, the relaxation rate becomes smaller and the Mössbauer nucleus can sense all the frozen moments of the nanoparticles exhibiting a well-resolved six-line pattern [Fig. 3(c)]. The spectrum is fitted with two hyperfine fields of 518 and 480 KOe and has been assigned to γ-Fe_2O_3 nanoparticles. The Mössbauer spectra of the sample 4 are very similar to that of the sample 3 and have

TABLE I. ^{57}Fe Mössbauer parameters of maghemite and cobalt-ferrite nanoparticles embedded in polystyrene resin.

		Hyperfields (kOe)						
Sample[a]	Temp. (K)	H_1	H_2	IS (δ) (mm/s)	QS (Δ) (mm/s)	LW (mm/s)	Assignments	M_s (emu/cm^3)
1	300	482	443	0.24	0.35	0.93	γ-Fe_2O_3	325
	78	517	488	0.24		0.66	γ-Fe_2O_3	
2	300	492	453	0.24	0.35	0.47	SP $Co_xFe_{3-x}O_4$ (x=0.6)	310
	78	528		0.12		0.61	$Co_xFe_{3-x}O_4$ (x=0.6)	
3	300	⋯	⋯	0.11	0.36	0.42	SP γ-Fe_2O_3	260
	4.2	518	480	0.13		0.65	γ-Fe_2O_3	
4	300	521	481	0.14	0.37	0.58	SP-$Co_xFe_{3-x}O_4$ (x=0.3)	227
	4.2			0.12		0.59	$Co_xFe_{3-x}O_4$ (x=0.3)	

[a]See text for sample description, SP-superparamagnetic.

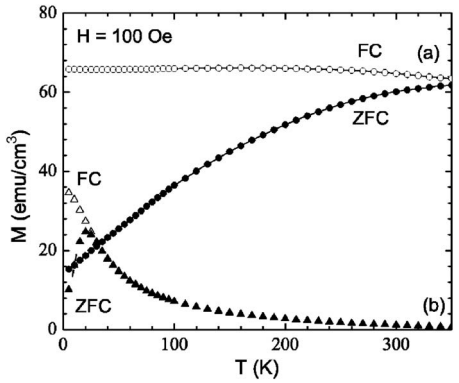

FIG. 4. ZFCM and FCM curves for samples (a) 1 and (b) 3.

been attributed to $Co_xFe_{3-x}O_4$ with $x=0.3$. It is important to note that both γ-Fe_2O_3 and $Co_xFe_{3-x}O_4$ have a spinel, AB_2O_4, structure and therefore produce identical x-ray-diffraction pattern and Mössbauer spectrum. However, due to the greater sensitivity for detecting minute changes in the chemical environment, Mössbauer effect can distinguish between γ-Fe_2O_3 and $Co_xFe_{3-x}O_4$ phases by detecting small changes in the hyperfine fields. It is noteworthy that the amount to Co introduced in the spinel phase of sample 4 (synthesized by using ferric ions) is less than that for sample 2 (synthesized by using the ferrous ions) under the identical reaction conditions. This perhaps is due to the fact that there are more divalent sites than the trivalent in the resin matrix. This provides greater opportunity for ferrous ions to react with Co than the ferric ions. Table I lists all the Mössbauer parameters for the samples.

The zero-field-cooled magnetization (ZFCM) measurement curve for sample 1 shows broad maxima [Fig. 4(a)] in comparison with the sample 3 [Fig. 4(b)]. The corresponding temperatures of ~350 and 20 K represent their respective blocking temperatures (T_B). Figure 5 shows the ZFCM and FCM curves for samples 2 and 4. The nature of the curves remain similar, however, the blocking temperature increases to >350 and 38 K for these two samples. Therefore, by introducing Co in the γ-Fe_2O_3 resin matrix, the particle size and hence the blocking temperature are increased. However, the increase in blocking temperature could as well be due to

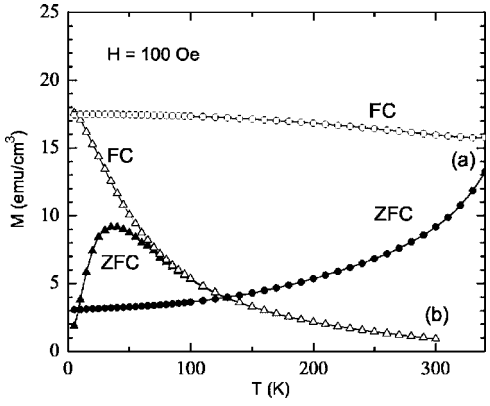

FIG. 5. ZFCM and FCM curves for samples (a) 2 and (b) 4.

an increase in the anisotropy constant of cobalt-ferrite nanoparticles. Furthermore, a plot of inverse susceptibility versus temperature data for $T>T_B$ did not follow a Curie behavior in the case of samples 3 and 4, suggesting the presence of intra- and/or interparticle interaction. However, one needs to consider the temperature dependence of the saturation magnetization, M_s, to accurately elucidate particle interaction.

The M-H curves at 300 K show a remanence and coercivity for the samples 1 and 2 and no remanence and coercivity for samples 3 and 4. However, hysteresis did occur below T_B for all the samples. This result is in agreement with the Mössbauer measurement which shows a six-line pattern corresponding to a majority of blocked moments (80% of the spectral area) for samples 1 and 2 and a quadruple doublet corresponding to the unblocked moments for samples 3 and 4 at 300 K. The M_s values were estimated from the curves at 5 K and are listed in Table I. Notably, the M_s values for all the samples are smaller than the bulk value[12] of 410 emu/cm^3 for γ-Fe_2O_3. Sato *et al.*[13] have found that the saturation magnetization of ferrite nanoparticles decreases sharply below 10 nm size owing to crystalline magnetic anisotropy. Other studies by Coey[14] and Morup[15] have shown that nonlinear spin structure could give rise to spin pinning and a reduced magnetic moment of the particles.

In summary, we have synthesized cobalt-ferrite nanoparticles by ion-exchange method and studied their structural and magnetic properties. The size of the nanoparticles, the composition of the Fe–Co ferrites, and the blocking temperatures were found to depend upon whether divalent or trivalent Fe was used in the synthesis. The divalent Fe favors larger particle size, higher blocking temperature, and higher amount of Co in the ferrites than the trivalent Fe.

ACKNOWLEDGMENT

This work has been supported by NSF Grant No. DGE 9870720.

[1] A. T. Ngo and M. P. Pileni, J. Phys. Chem. B **105**, 53 (2001).
[2] M. H. Sousa and F. A. Tourinbo, J. Phys. Chem. B **105**, 1168 (2001).
[3] C. C. Berry, S. Wells, S. Charles, and A. S. G. Curtis, Biomaterials **24**, 4551 (2003).
[4] C. T. Black, C. B. Murray, R. L. Sandstorm, and S. Sun, Science **290**, 1131 (2000).
[5] R. F. Ziolo, E. P. Giannelis, B. A. Weinstein, M. P. O'Horo, B. N. Ganguly, V. Mehrotra, M. W. Russell, and D. R. Huffman, Science **257**, 5067 (1992).
[6] G. M. Tsoi, U. Senaratne, R. J. Tackett, E. C. Buc, R. Naik, P. P. Vaishnava, V. M. Naik, and L. E. Wenger, J. Appl. Phys. **97**, 10J507 (2005); Phys. Rev. B **72**, 014445 (2005).
[7] R. Naik *et al.*, J. Magn. Magn. Mater. **272–276**, E1239 (2004).
[8] R. Naik, U. Senaratne, N. Powell, E. C. Buc, G. M. Tsoi, V. M. Naik, P. P. Vaishnava, and L. E. Wenger, J. Appl. Phys. **97**, 10J313 (2005).
[9] U. O. Hafeli, S. M. Sweeney, and B. A. Beresford, Nucl. Med. Biol. **22**, 147 (1995).
[10] U. O. Hafeli and G. J. Pauer, J. Magn. Magn. Mater. **194**, 76 (1999).
[11] A. J. Rondione, A. C. S. Samia, and Z. J. Zhang, Appl. Phys. Lett. **76**, 3624 (2000).
[12] R. W. Chantrell, J. Popplewell, and S. Charles, IEEE Trans. Magn. **MAG-14**, 975 (1978).
[13] T. Sato, T. Iijima, M. Sekin, and N. Inagaki, J. Magn. Magn. Mater. **65**, 252 (1987).
[14] M. D. Coey, Phys. Rev. Lett. **27**, 1140 (1971).
[15] S. Morup, J. Magn. Magn. Mater. **39**, 45 (1983).